AMSI SUMMER RESEARCH SCHOLARSHIPS 2024–25

Get a taste for Research this Summer

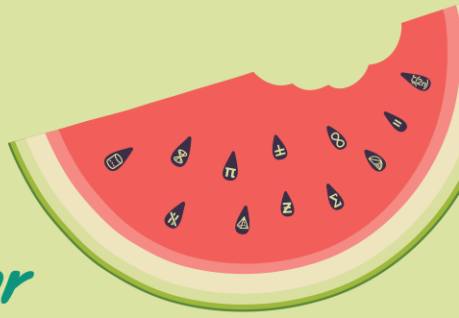

Introducing Calcium into Mathematical Models for Atherosclerosis

Faith Sawers

Supervised by Associate Professor Edward Green and Professor Yvonne Stokes

University of Adelaide

Jane Street®

AMSI AUSTRALIAN MATHEMATICAL SCIENCES INSTITUTE

Abstract This report presents an ordinary differential equation (ODE) model in which the process of calcification in atherosclerosis is exhibited for the most basic case. The model builds upon the previous ODE model built in *Athero-protective Effects of High Density Lipoproteins (HDL): An ODE Model of the Early Stages of Atherosclerosis* presented by Anna Cohen, Mary Myerscough, and Rosemary Thompson in 2014. The new model specifically builds on the results of this paper to include calcification. Calcification in atherosclerosis is associated with both rupture and stabilisation of plaque. The investigation of the created model through graphical analysis supports the dichotomy observed in the biology.

1 Introduction

Atherosclerosis is a cardiovascular disease of the heart distinguished by the formation of a fatty streak, also called plaque, in the arterial walls that contain lipids and cellular debris. In the centre of the plaque, foam cells and lipid droplets form a core region that is surrounded by a cap of smooth muscle cells and a collagen-rich matrix. The fibrous cap prevents contact between the blood and the pro-thrombotic material in the lesion. Disruption of the cap can lead to thrombosis, instigating a heart attack or stroke (Hansson & Libby, 2006).

Atherosclerosis can also regress with time, with detection and treatment, thus significantly reducing the chance of a heart attack or stroke (Arsenault *et al.*, 2012).

A 2022 National Health Survey found that 6.7% of Australia's adult population were living with one or more conditions related to heart, stroke, and vascular disease (Australian Institute of Health and Welfare, 2024).

Calcification of the coronary arteries occurs via an active process that resembles bone formation under complex enzymatic and cellular pathways (Alexopoulos & Raggi, 2009). Microcalcifications, but not large calcifications, are harmful. Calcification is a hallmark of atherosclerosis (Nakahara *et al.*, 2017), and is believed to profoundly affect plaque stability, largely due to the coronary artery calcium (CAC) score predicting cardiovascular mortality (Kawtharany *et al.*, 2022).

The aim of this paper is to develop a simple system of ordinary differential equations (ODEs) to model the process of calcification in atherosclerosis. As atherosclerosis is quite prevalent in Australia, it is useful to investigate this disease and calcium's role in plaque rupture.

The new system of ODEs will be built upon Cohen *et al.* (2014). This system will be solved numerically and analysed graphically to determine if the different outcomes of calcification in atherosclerosis can be represented clearly.

2 Statement of authorship

Under the direction of Associate Professor Edward Green, Faith developed and analysed the model presented in this report. The model was extended from Cohen *et al.* (2014) paper titled, *Athero-protective Effects of High Density Lipoproteins (HDL): An ODE Model of the Early Stages of Atherosclerosis.*

3 Biological background

First, to introduce calcium into a pre-existing mathematical model for atherosclerosis, a thorough review of literature to understand atherosclerosis, calcification in atherosclerosis, and the mathematical models that already exist.

3.1 Atherosclerosis

3.1.1 Relevance of atherosclerosis

Atherosclerosis is the buildup of fats, cholesterol, and other substances in and on the artery walls. This buildup, called plaque, causes the arteries to narrow, blocking blood flow. This plaque can also burst, leading to a blood clot which can cause an acute cardiac event such as a heart attack or a stroke (Mayo Clinic Staff, 2024). Atherosclerosis can cause some types of cardiovascular disease , (Australian Institute of Health and Welfare, 2024). A 2022 National Health Survey found that 6.7% of Australia's adult population were living with one or more conditions related to heart, stroke, and vascular disease (Australian Institute of Health and Welfare, 2024).

3.1.2 In depth biological explanation of atherosclerotic lesion formation

Atherosclerotic lesions begin to form when low density lipoproteins, LDL, enter the artery lining are oxidised or modified to be modLDL (Hansson & Libby, 2006). LDL is more colloquially known as 'bad' cholesterol. These modLDL present in the *intima*, the innermost layer of the artery, activating an inflammatory response. This inflammatory response attracts monocytes, which enter through the endothelial cell wall (Libby, 2002). It then can involve other inflammatory cells, including T-cells and mast cells, but initially only involves monocyte-derived macrophages (Tabas, 2010). Once inside the arterial intima, these monocytes differentiate into *macrophages*, a type of white blood cell, which bind to the modLDL (Tabas, 2010).

For large concentration of modLDL, the macrophages become lipid laden, and produce a foam cell (Libby, 2002). They are called foam cells as when observed under a microscope, they exhibit a foamy appearance.

Efferocytosis, the process by which apoptotic tissue is recognised for engulfment by phagocytic cells such as macrophages, is inhibited in atherosclerotic plaque (Kojima *et al.*, 2017). In early atherosclerotic plaque, this process is able to occur successfully and remove foam cells and other necrotic material from the intima. However, as the lesion progresses, this process begins to fail (Tabas, 2010).

When these foam cells are lipid laden, they lose their ability to undergo efferocytosis and escape back into the blood stream or lumen. Macrophages and foam cells then congregate in a central core in the atherosclerotic plaque, where they can die, producing the necrotic core in the lesion (Libby, 2002). This plaque can become unstable and burst. This process is shown in figure 1.

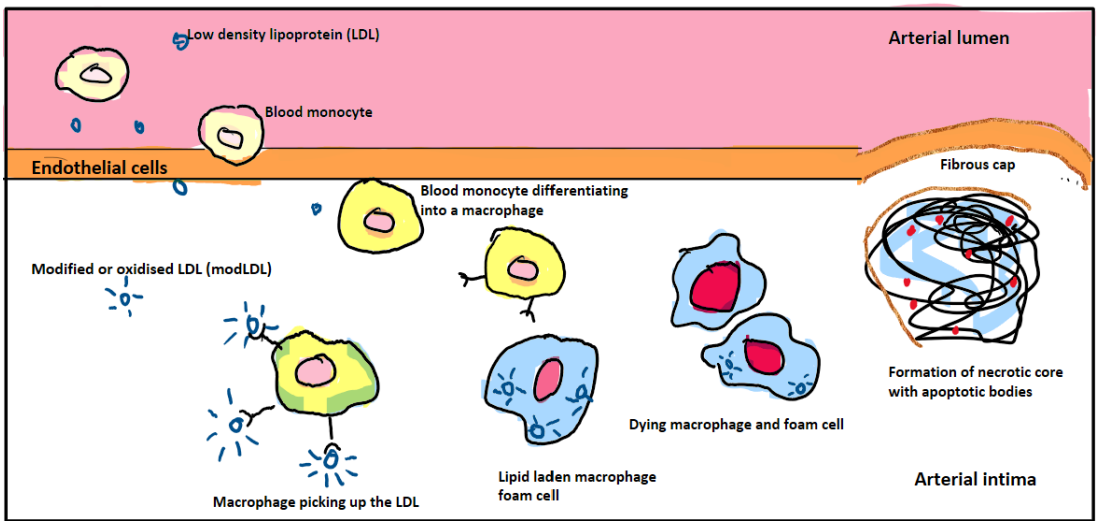

Figure 1: Figure displaying the process of atherosclerosis, read from left to right as time progresses.

3.2 Calcification

As atherosclerosis progresses, calcium development occurs within these lesions (Andrews *et al.*, 2018). The calcification process of the arteries, and of atherosclerotic plaque, is now widely regarded as an active process, stimulated by inflammatory pathways (Andrews *et al.*, 2018) (Shioi & Ikari, 2018).

3.2.1 Types of calcification

There are 3 types of calcification: Microcalcification, Spotty calcification, and Macrocalcification (Shi *et al.*, 2020). Sometimes microcalcification and spotty calcification are considered analogous (Shioi & Ikari, 2018) which is the assumption adapted for this model.

3.2.2 Microcalcification

Microcalcifications may represent an early stage in the progression into vascular calcification (Shi *et al.*, 2020). Microcalcifications coalesce into large masses, extending from the deeper region of the necrotic core into the surrounding matrix, and finally form calcified sheets or plates (Yahagi *et al.*, 2016). These are the macrocalcifications.

3.2.3 Macrocalcification

Macrocalcification is thought to occur during the healing phase of an atherosclerotic lesion, inducing the resolution of inflammation via facilitating plaque calcification that facilitates plaque calcification (Shioi & Ikari, 2018). They are larger than microcalcifications.

3.2.4 In depth biological explanation of calcification formation

In simplified terms, according to Shi *et al.* (2020) and Shioi & Ikari (2018), calcification is formed after macrophage and foam cell death occurs in an atherosclerotic lesion, where apoptotic bodies and matrix vesicles are released from the deaths. These vesicular structures act as sites for calcium phosphate crystal formation, and microcalcification begins to occur at these many different sites.

Plaque calcification is thought to be developed by the inflammation-dependent mechanisms involved in progression and regression of atherosclerosis (Shioi & Ikari, 2018). Microcalcification is understood to have pro-inflammatory properties, and macrocalcification to have anti-inflammatory properties (Shioi & Ikari, 2018).

3.2.5 Relevance of calcification to atherosclerotic region stability

Calcification of coronary arteries has been directly correlated with *atheroma volume*, more commonly referred to as plaque volume, in a large pathological study of human coronary arteries (Andrews *et al.*, 2018).

Macrocalcification has an inverse correlation to plaque rupture (Andrews *et al.*, 2018)(Shioi & Ikari, 2018). Microcalcification is more likely to be associated with a plaque rupture. (Andrews *et al.*, 2018)(Shioi & Ikari, 2018). Furthermore, microcalcifications in atherosclerotic plaque have been demonstrated to be related to plaque vulnerability (Shi *et al.*, 2020). This supports the recent studies that suggests that not all vascular calcification indicates an equivalent atherosclerotic risk, when taking into account distribution and shape of plaque calcification (Andrews *et al.*, 2018).

According to biomechanical analysis, plaque rupture occurs at highly stressed sites. In general, stress concentration is greatly increased at interfaces between rigid and compliant structures such as between calcium material and normal arterial wall or fibrous plaque (Demer *et al.*, 1994).

As seen in figure 2, there are two recognised pathways s that microcalcifications lead to plaque rupture:

- Inflammatory cytokines from macrophages activating osteogenic differentiation, leading to early stages of calcification, from which a **positive feedback loop between inflammation and calcification** produces microcalcification, stimulating accelerated plaque burden and a larger necrotic core, (Shi *et al.*, 2020) seen in the vertical path of figure 2.

- Calcification at the lipid pool, especially near the fibrous cap, increasing stress levels and causing a plaque rupture (Shi *et al.*, 2020), seen in figure 2's downward path.

Investigating how these calcifications form, and progress, is useful for understanding why a rupture occurs and how to prevent them in the future. Creating a system to model this process can also help create a deeper understanding of calcium's unique role in microcalcification correlating with plaque rupture and macrocalcification correlating with plaque stabilisation.

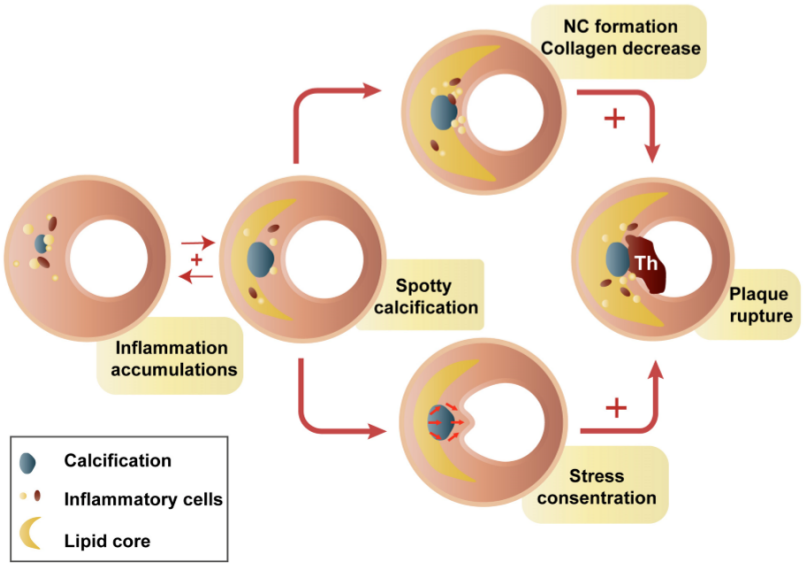

Figure 2: Figure from Shi *et al.* (2020) displaying hypothesis of how micro (spotty) calcification interacts with plaque rupture. NC: necrotic core, Th: thrombus (a blood clot).

4 Developing the model

4.1 Existing Mathematical Models

To create the new model, the system presented in Cohen *et al.* (2014) was extended. Cohen *et al.* (2014) focused on lipid content in early-stage atherosclerosis. This model was selected as the basis as its system consists of three state variables- modLDL, macrophages, and foam cells- which are also important in initial calcification. It therefore makes biological sense to include calcification in this model. In this model,

- $l(t)$ represents the concentration of modLDL in the intima at time t,
- $m(t)$ is the capacity of active macrophages in the intima to ingest modLDL at time t,
- and $n(t)$ is internalised lipid content in foam cells at time t.

m can be thought of more broadly as macrophage content, and n as foam cell content. An increase in inflammation can be understood of as an increase of m content.

In addition to the assumptions made in Cohen *et al.* (2014), the following assumptions were added:

1. Necrosis and apoptosis that leads to calcification depends only on foam cells, $n(t)$.
2. Necrosis and apoptosis that leads to calcification occurs at a constant rate.

The new, dimensional model is shown in Equations 1-4 where the black text is from Cohen *et al.* (2014) and the red text is the new additions.

Please observe that there are some constant functions in the system of equations that are in terms of ℓ and h. This is related to LDL ("bad" cholesterol) and HDL ("good" cholesterol). These are assumed to be constant on the time scale of the model. ℓ and h are treated as parameters in the model.

A system state, $c(t)$, is added to Cohen *et al.* (2014). This represents the microcalcification content. The new constants and rate functions are added as well which are included in the table.

$$\frac{d\ell}{dt} = \underbrace{-aU(\ell)m}_{\substack{\text{removal}\\ \text{of modLDL}}} + \underbrace{K(h)}_{\substack{\text{modLDL}\\ \text{influx}}} + \underbrace{\lambda_1 n}_{\substack{\text{modLDL influx}\\ \text{from apoptosis}\\ \text{and necrosis}}}, \tag{1}$$

The first term in the right-hand-side (RHS) of Equation 1 represents the modLDL consumed by macrophages, and the second term represents the influx of modLDL from the arterial lumen into the arterial intima. $K(h)$ is chosen to be some smooth positive, decreasing function. The third term on the RHS of Equation 1 represents the lipid released into the intima from the apoptosis and necrosis of foam cells.

$$\frac{dm}{dt} = \underbrace{-c_a U(\ell)m}_{\substack{\text{reduction in}\\ \text{macrophage}\\ \text{capacity}}} + \underbrace{r_m R(h)n}_{\substack{\text{recycled}\\ \text{capacity}}} - \underbrace{a_m A(l,h)m}_{\substack{\text{macrophage}\\ \text{emigration}}} + \underbrace{D(h)\ell + f(h)\ell m}_{\substack{\text{macrophage}\\ \text{influx}}} + \underbrace{\lambda_3 cm(1-\frac{m}{\kappa_m})}_{\substack{\text{positive feedback}\\ \text{loop of calcium}\\ \text{stimulating inflammation}}}, \tag{2}$$

Equation 2 represents the change of macrophage content over time. The first term on the RHS represents the reduction in macrophage capacity from the conversion of macrophages to foam cells.

The second term is more complicated, representing the macrophages that are able to absorb modLDL, leave the intima, and return as macrophages. This works in tandem with the second term in Equation 3. From Cohen *et al.* (2014), it is assumed that the rate at which capacity can be reused is at most as fast as the rate at which the lipid is removed by HDL so $r_m \leq r_n$.

The third term on the RHS represents the macrophages that emigrate out of the intima.

The fourth and fifth terms on the RHS represent the influx of macrophages that are attracted due to the endothelial response to modLDL and those that are attracted due to the endothelial response to active macrophages.

The new RHS term represents the positive feedback loop between microcalcification and inflammation, specifically highlighting that an increase in microcalcification leads to an increase in macrophages.

$$\frac{dn}{dt} = \underbrace{dU(\ell)m}_{\substack{\text{internalised}\\ \text{modLDL}}} - \underbrace{r_n R(h)n}_{\substack{\text{cholesterol}\\ \text{efflux}}} - \underbrace{a_n B(l,h)n}_{\substack{\text{foam cell}\\ \text{emigration}}} - \underbrace{nN}_{\substack{\text{foam cells}\\ \text{forming the}\\ \text{necrotic core}}}, \tag{3}$$

In equation 3, the first term on the RHS represents that macrophages which have internalised modLDL and become foam cells. The second works in conjunction with the second RHS term in equation 2. The third represents the foam cells that are able to perform their biological function and can emigrate out of the intima.

The final term on the RHS is meant to represent the foam cells that undergo apoptosis and necrosis. This aligns with the assumption that only foam cells undergo apoptosis and necrosis.

$$\frac{dc}{dt} = \underbrace{\lambda_2 n}_{\substack{\text{calcification occurring}\\ \text{on apoptotic material}}} + \underbrace{c_r mc(1 - \frac{c}{\kappa_c})}_{\substack{\text{positive feedback}\\ \text{loop of inflammation}\\ \text{stimulating calcification}}} \tag{4}$$

Equation 4 is entirely new additions. The first term on the RHS represents the microcalcification that occurs from the necrosis and apoptosis of foam cells. This is separate from N defined earlier as the necrotic core is not entirely calcification. The second term represents the positive feedback loop between calcification and inflammation, focusing on how greater levels of inflammation promotes calcification content. For increased calcification content, this can represent more calcifications, which suggests instability (Shi *et al.*, 2020). It could also represent the microcalcifications coalescing together to form a macrocalcification. However, it is difficult to distinguish between which outcome occurs.

Therefore, the model can be improved through clearer definition of microcalcification resulting in instability versus microcalcification coalescing into macrocalcification. However, there appears to be a gap in the literature for why this difference occurs.

4.2 Nondimensionalised model and scalings

$$\frac{d\ell}{dt} = \underbrace{-U(\ell)m}_{\substack{\text{removal}\\ \text{of modLDL}}} + \underbrace{K(h)}_{\substack{\text{modLDL}\\ \text{influx}}} + \underbrace{\lambda_1 n}_{\substack{\text{modLDL influx}\\ \text{from apoptosis}\\ \text{and necrosis}}} \tag{5}$$

$$\frac{dm}{dt} = \underbrace{-U(\ell)m}_{\substack{\text{reductionin}\\ \text{macrophage}\\ \text{capacity}}} + \underbrace{r_m R(h)n}_{\substack{\text{recycled}\\ \text{capacity}}} - \underbrace{a_m A(l,h)m}_{\substack{\text{macrophage}\\ \text{emigration}}} + \underbrace{D(h)\ell + f(h)\ell m}_{\substack{\text{macrophage}\\ \text{influx}}} + \underbrace{\lambda_3 mc(1-m)}_{\substack{\text{positive feedback}\\ \text{loop of calcium}\\ \text{stimulating inflammation}}} \tag{6}$$

Table 1: Parameter Interpretation for existing and introduced parameters, with black text representing existing definitions from Cohen *et al.* (2014) and red text representing the new additions.

Parameter Interpretation	
Parameter	**Interpretation**
a	Maximum uptake rate of modLDL by macrophages.
c_a	Maximum rate of reduction in capacity of macrophages as a result of modLDL uptake.
d	Maximum rate of accumulation of internalised lipid in foam cells.
a_m	Maximum rate of emigration of macrophages.
a_n	Maximum rate of emigration of internalised lipid via foam cell emigration.
r_m	Maximum rate of return of active macrophage capacity as a result of cholesterol efflux from cells.
r_n	Maximum rate of cholesterol efflux out of foam cells.
N	Rate at which necrotic and apoptotic core is formed. Positive constant.
c_r	Rate of microcalcification. Positive constant.
κ_m	Maximum capacity of macrophages to provide inflammation. Positive constant.
κ_c	Maximum capacity of calcification to provide inflammation. Positive constant.
λ_1	Rate that lipid is released from the necrosis and apoptosis of the foam cells, positive constant.
λ_2	Rate at which necrosis and apoptosis lead to the microcalcification occurring at the many sites of these deaths, positive constant.
λ_3	Strength of positive feedback loop between microcalcification and inflammation, positive constant.

$$\frac{dn}{dt} = \underbrace{U(\ell)m}_{\substack{\text{internalised}\\ \text{modLDL}}} - \underbrace{r_n R(h)n}_{\substack{\text{cholesterol}\\ \text{efflux}}} - \underbrace{a_n B(l,h)n}_{\substack{\text{foam cell}\\ \text{emigration}}} - \underbrace{nN}_{\substack{\text{foam cells}\\ \text{forming the}\\ \text{necrotic core}}} \tag{7}$$

$$\frac{dc}{dt} = \underbrace{\lambda_2 n}_{\substack{\text{calcification occurring}\\ \text{on apoptotic material}}} + \underbrace{c_r m c(1-c)}_{\substack{\text{positive feedback}\\ \text{loop of inflammation}\\ \text{stimulating calcification}}} \tag{8}$$

4.2.1 Scalings

The following scalings were utilised to achieve this result:

$$\hat{\ell} = \ell, \quad \hat{m} = \frac{am}{c_a}, \quad \hat{n} = \frac{an}{d}, \quad \hat{t} = ct, \quad \hat{K(h)} = \frac{K(h)}{c_a}, \quad \hat{D(h)} = \frac{D(h)a}{c_a^2},$$

$$\hat{f(h)} = \frac{f(h)}{c_a}, \quad \hat{r_m} = \frac{dr_m}{c_a^2}, \quad \hat{r_n} = \frac{r_n}{c_a}, \quad \hat{a_m} = \frac{a_m}{c_a}, \quad \hat{a_n} = \frac{a_n}{c_a}$$

These were the same as given in Cohen *et al.* (2014). And introduced scaling parameters

$$\hat{\lambda_1} = \frac{d\lambda_1}{c_a a}, \quad \hat{\lambda_2} = \frac{d\lambda_2}{ca\kappa_c}, \quad \hat{\lambda_3} = \frac{\kappa_c \lambda_3}{c_a}, \quad \hat{c_r} = \frac{c_r}{a}$$

To make the most simplified model, it was set

$$a_m = a_n = 0.$$

This represents the scenario in which there is no emigration occurring by macrophages and foam cells. And,

$$r_m = r_n = 0.$$

This represents the scenario in which once a macrophage has become a foam cell, it cannot revert back to a macrophage.

Both of these scenarios are reasonable to assume over a small time scale.

Suitable functions were chosen to represent the constant functions and parameters from Cohen *et al.* (2014). These are in black text in Table 2. For the new additions, we set the parameter $N = 1$. This is because N must be present for calcification to occur (Shioi & Ikari, 2018). It is also set that $c_r = 1$. These are in red text in Table 2. Equation (5) to equation (8) were next substituted into MATLAB and solved over a small time scale using an ode solver.

Table 2: Parameter and Constant Function Values

Parameter or Constant Function	**Chosen Value**
$U(\ell)$	$\frac{l^2}{1+l^2}$
$K(h)$	5
$R(h)$	1
$A(\ell, h)$	1
$B(\ell, h)$	1
$D(h)$	2
$f(h)$	0.3
a_m	0
a_n	0
r_m	0
r_n	0
N	1
c_r	1

5 Results

First, it was investigated how individual λ impacted the system when compared to Cohen *et al.* (2014).

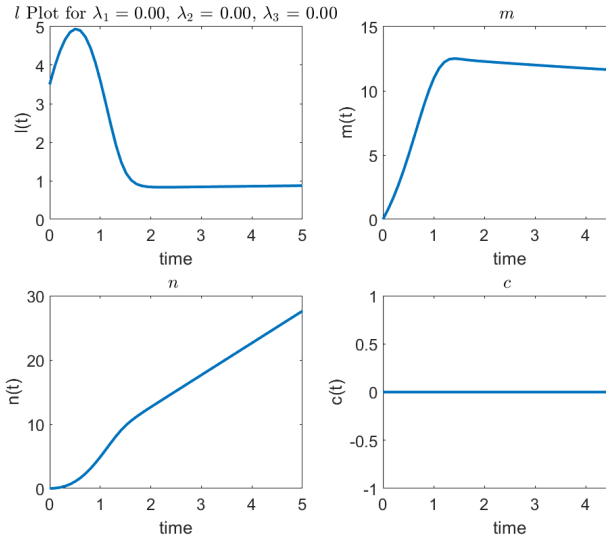

Figure 3: Results from Cohen *et al.* (2014).

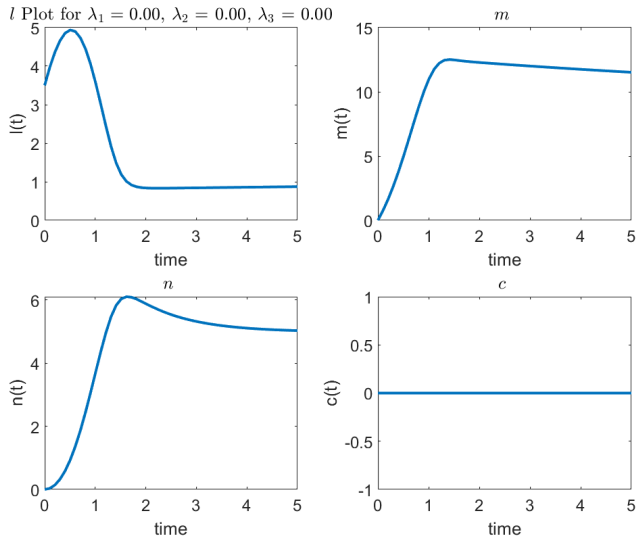

Figure 4: Results from new model with $N = 1, c_r = 1$

5.1 Comparing New Model with Cohen *et al.* (2014)'s results

Introducing calcification when compared to the 2014 model shows displayed in comparing figure 3 to figure 4 the foam cell content $n(t)$ decreasing. This represents the foam cells dying and beginning to form the necrotic core where the calcification sites are. This difference is because figure 3 does not take into account foam cell death from apoptosis and necrosis like figure 4.

Next, it was investigated how the system behaved for each λ being activated individually.

5.2 Case for when activating only modLDL influx from apoptosis and necrosis of foam cells

For increasing λ_1, and leaving all other λ=0, this impacts $m(t)$ as seen in figure 6. This increase makes the macrophage capacity begin to increase dramatically, where it previously stabilised like in figure 5. It also causes the lipid content $l(t)$ to have a peak and valley before entering a steady state in figure 6. It also causes the foam cell content to increase linearly and become unstable. This is expected as increasing λ_1 increases the lipid, so more macrophages will come to the lesion site, in and possibly become foam cells. Therefore, for larger λ_1, we expect a higher likelihood of an unstable plaque.

5.3 Case for when activating only initial calcification on apoptotic material.

For increasing λ_2, leaving $\lambda_1 = \lambda_3 = 0$ seen in figure 8 when compared to figure 7, this impacts $c(t)$. Figure 8 shows the calcium content spike up and then reaches a steady state. This represents the calcification formation. This is an expected observation, as for increased λ_2 we have increased calcium formation as there is more apoptotic material for initial sites to occur.

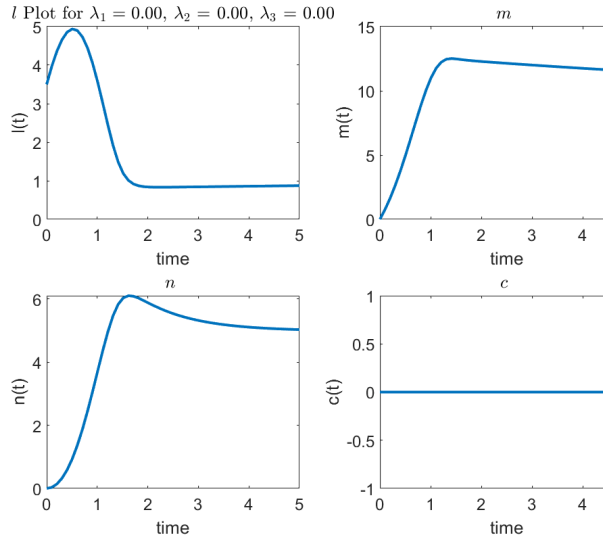

Figure 5: Results when leaving $\lambda_1 = \lambda_2 = \lambda_3 = 0, N = 1, c_r = 1$.

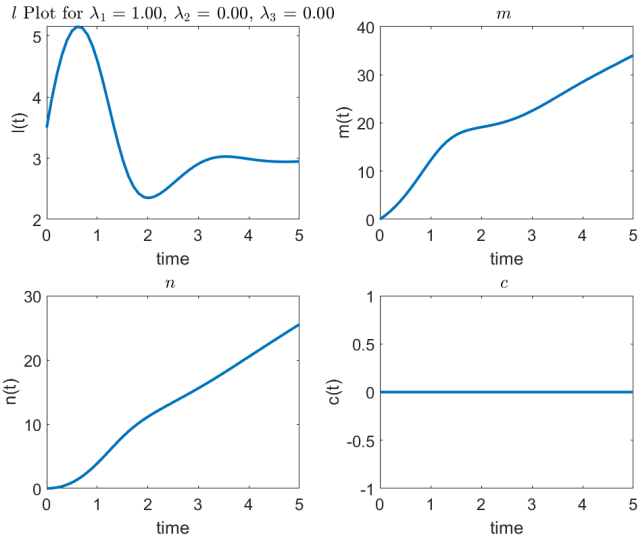

Figure 6: Results when increasing $\lambda_1 = 1$, leaving $\lambda_2 = \lambda_3 = 0, N = 1, c_r = 1$.

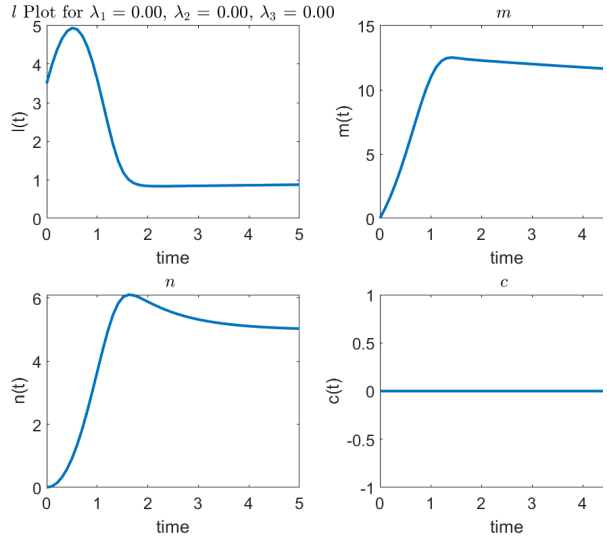

Figure 7: Results when leaving $\lambda_1 = \lambda_2 = \lambda_3 = 0, N = 1, c_r = 1$

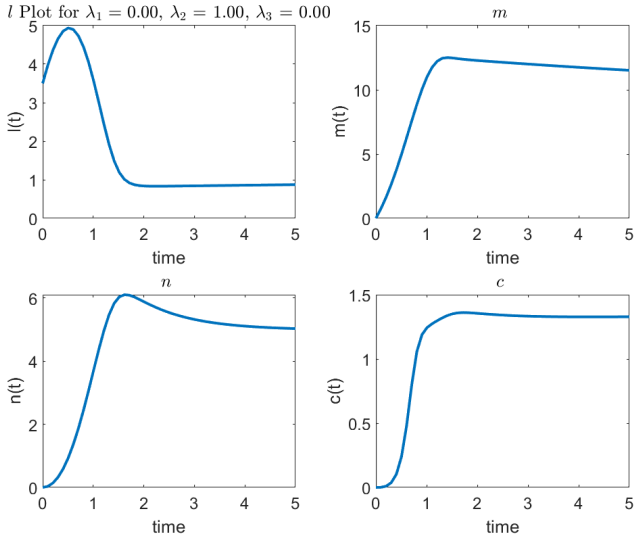

Figure 8: Results when increasing $\lambda_2 = 1$, leaving $\lambda_1 = \lambda_3 = 0, N = 1, c_r = 1$

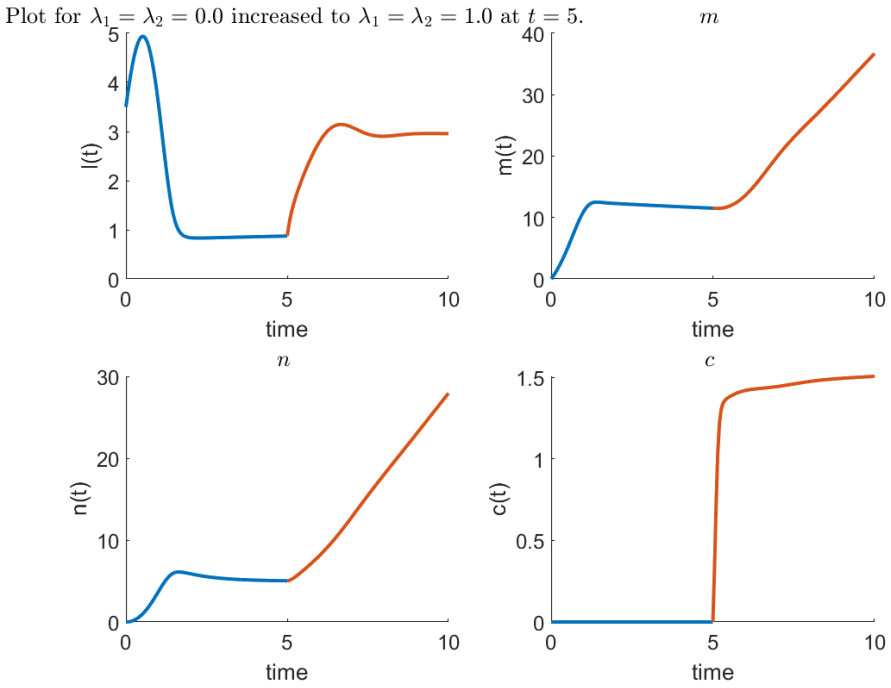

Figure 9: Plots of l, m, n, c change for $\lambda_1 = \lambda_2 = 1$, $\lambda_3 = 0$ introduced at $t = 5$. Over the whole plot $N = 1, c_r = 1$. This plot shows the calcification increase align with plaque destabilisation.

5.4 Case for when activating only feedback loop between macrophages and calcification.

Now, increasing λ_3 and leaving $\lambda_1 = \lambda_2 = 0$ does not change the overall concentration of l, m, n, c. This is expected as λ_3 cannot be meaningful unless λ_2 is present, as the feedback loop between inflammation and calcification cannot occur without calcification.

Now, we will examine the **system for when λ_2 is introduced at $t = 5$ in conjunction with λ_1 and λ_3.**

5.5 Case for when modLDL influx from foam cell death and initial calcification are activated

First, the case where $\lambda_1 = \lambda_2 = 1$ and $\lambda_3 = 0$ is exhibited in figure 9. Figure 9 displays that the plaque clearly becomes unstable as $n(t), m(t)$ begin to increase linearly for $t > 5$. Also for $t > 5$, the lipid content appears to reach a second equilibrium after its steady state is disrupted. The calcium content also increases suddenly for $t > 5$, and then continues to increase slowly after reaching $c(t) = 1.5$. It is expected that the macrophage and calcium content would continue to grow in this case as the inflammation-calcification feedback loop is activated for $c(t)$. Larger λ_1 increases modLDL content and therefore also increaases macrophage and foam cell content. This supports the biological observation of calcification being present in plaque destabilisation. Furthermore, a

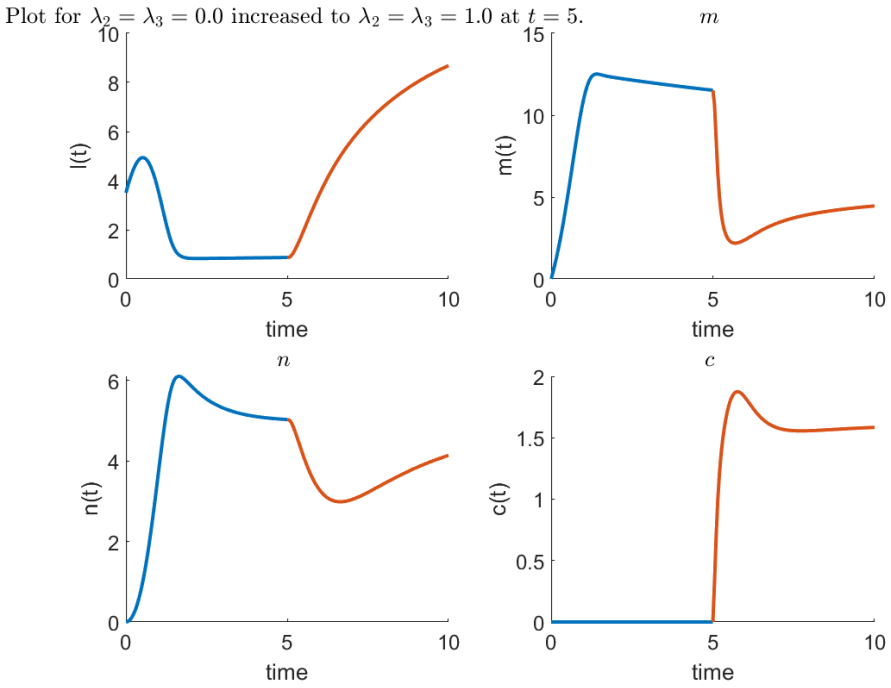

Figure 10: Plots of l, m, n, c change for $\lambda_2 = \lambda_3 = 1$, $\lambda_1 = 0$ introduced at $t = 5$. Over the whole plot $N = 1, c_r = 1$. This plot shows the increase of calcification align with plaque stabilisation.

study investigating the relationship between plaque inflammation and calcification suggested that inflammation in atherosclerotic plaque may precede active calcification. (Dweck *et al.*, 2016) Therefore, we would expect to see an increase in inflammation, or in this case, $m(t)$, before calcification occurs. This is observed in figure 9 as $t < 5$ has $m(t) > 0$.

5.6 Case for when initial calcification and the feedback loop between calcium and inflammation are both activated.

For the case displayed in figure 10, $\lambda_2 = \lambda_3 = 1$, $\lambda_1 = 0$. When $t > 5$, the lipid content begins to grow significantly, stabilising at a greater t. The calcium content increases drastically and then reaches a steady state. Both the foam cell and macrophage content drop, before beginning to slowly increase again until an equilibrium is reached for both foam cell and macrophage content. Figure 10 supports that both of these steady states are at a lower, and thus more stable, content level than for $t < 5$. The plaque here is stable. Therefore, this calcification is more likely to coalesce into a macrocalcification and not rupture. This also supports what we see in statins, a common medication for atherosclerosis, where statins drastically increase a patients calcium count while appearing to stabilise their atherosclerosis. (Andrews *et al.*, 2018).

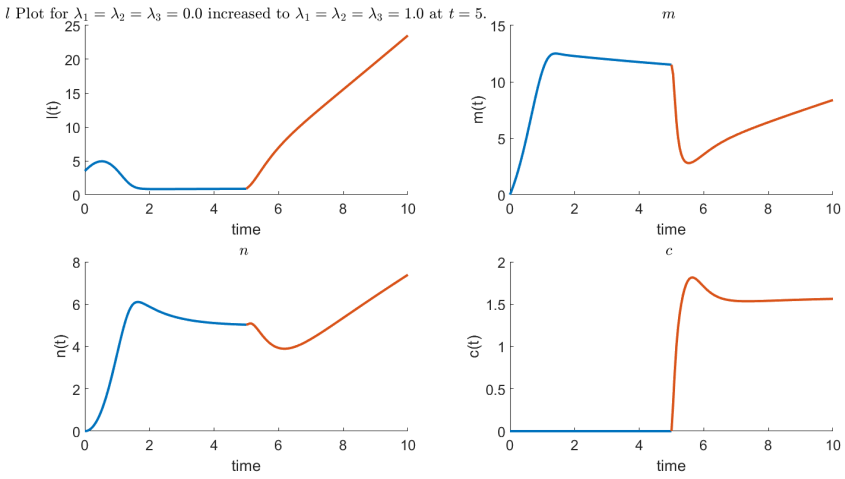

Figure 11: Plots of l, m, n, c change for $\lambda_1 = \lambda_2 = \lambda_3 = 1$ introduced at $t = 5$. Over the whole plot $N = 1, c_r = 1$. This plot shows the increase of calcification align with an extremely unstable plaque.

5.7 Case for when the modLDL influx from foam cell death, initial calcification, and the feedback loop between calcification and inflammation are activated

For all $\lambda_1, \lambda_2, \lambda_3$ being activated, figure 11 also shows the plaque becoming unstable. All lipid, macrophage, and foam cell content begin to increase linearly, with c content increasing drastically and then reach a quasi-equilibrium, where it continues to slowly increase due to the feedback loop between calcification and inflammation. Therefore, due to the large increase in content from all parameters, figure 11 represents a highly unstable plaque very likely to rupture.

6 Conclusion

It is clear from the model that the observation of microcalcification being associated with a rupture while also being the precursor for macrocalcification can coexist and be represented in a mathematical system. For the calcification to align with a macrocalcification and thus plaque calcification, λ_1 must be small. From extending Cohen *et al.* (2014), a new system of four ODEs was created to represent the process of microcalcification formation in atherosclerotic plaque. Through investigation, it was determined that there were cases of

- unstable plaque with steady calcification, as in Section 5.5,
- steady plaque with steady calcification, as in Section 5.6,
- unstable plaque with quasi-stable calcification, as in Section 5.7.

It is a point of interest to see how to distinguish between these cases in a clearer way. This could be achieved by improving the model to include the process of apoptosis and necrosis more clearly.

7 Acknowledgments

I'd like to thank the Australian Mathematical Sciences Institute (AMSI) for this scholarship. I'd like to especially thank my supervisor Associate Professor Edward Green, for his support and supervision. I am also sincerely grateful to Professor Yvonne Stokes for her insights and encouragement. I'd also like to thank Professor Mary Myerscough and Associate Professor Christina Bursill their invaluable contributions.

References

Alexopoulos, Nikolaos, & Raggi, Paolo. 2009. Calcification in atherosclerosis. *Nature Reviews Cardiology*, **6**(11), 681–688.

Andrews, Jordan, Psaltis, Peter J, Di Bartolo, Belinda A, Nicholls, Stephen J, & Puri, Rishi. 2018. Coronary arterial calcification: a review of mechanisms, promoters and imaging. *Trends in Cardiovascular Medicine*, **28**(8), 491–501.

Arsenault, Benoit J, Kritikou, Ekaterini A, & Tardif, Jean-Claude. 2012. Regression of atherosclerosis. *Current cardiology reports*, **14**, 443–449.

Australian Institute of Health and Welfare. 2024. *Heart, Stroke and Vascular Disease: Australian Facts*. Online. Accessed: 2025-02-03.

Cohen, Anna, Myerscough, Mary R, & Thompson, Rosemary S. 2014. Athero-protective effects of high density lipoproteins (HDL): an ODE model of the early stages of atherosclerosis. *Bulletin of mathematical biology*, **76**, 1117–1142.

Demer, Linda L, Watson, Karol E, & Boström, Kristina. 1994. Mechanism of calcification in atherosclerosis. *Trends in cardiovascular medicine*, **4**(1), 45–49.

Dweck, Marc R, Aikawa, Elena, Newby, David E, Tarkin, Jason M, Rudd, James HF, Narula, Jagat, & Fayad, Zahi A. 2016. Noninvasive molecular imaging of disease activity in atherosclerosis. *Circulation research*, **119**(2), 330–340.

Hansson, Göran K, & Libby, Peter. 2006. The immune response in atherosclerosis: a double-edged sword. *Nature reviews immunology*, **6**(7), 508–519.

Kawtharany, Lynn, Bessueille, Laurence, Issa, Hawraa, Hamade, Eva, Zibara, Kazem, & Magne, David. 2022. Inflammation and microcalcification: a never-ending vicious cycle in atherosclerosis? *Journal of Vascular Research*, **59**(3), 137–150.

Kojima, Yoko, Weissman, Irving L, & Leeper, Nicholas J. 2017. The role of efferocytosis in atherosclerosis. *Circulation*, **135**(5), 476–489.

Libby, P. 2002. Inflammation in Atherosclerosis. *Nature*, **420**(6917), 868–874.

Mayo Clinic Staff. 2024. *Arteriosclerosis/Atherosclerosis*. Online. Accessed: 2025-02-01.

Nakahara, Takehiro, Dweck, Marc R, Narula, Navneet, Pisapia, David, Narula, Jagat, & Strauss, H William. 2017. Coronary artery calcification: from mechanism to molecular imaging. *JACC: Cardiovascular Imaging*, **10**(5), 582–593.

Shi, Xuan, Gao, Jie, Lv, Qiushi, Cai, Haodi, Wang, Fang, Ye, Ruidong, & Liu, Xinfeng. 2020. Calcification in atherosclerotic plaque vulnerability: friend or foe? *Frontiers in physiology*, **11**, 56.

Shioi, Atsushi, & Ikari, Yuji. 2018. Plaque calcification during atherosclerosis progression and regression. *Journal of atherosclerosis and thrombosis*, **25**(4), 294–303.

Tabas, Ira. 2010. Macrophage death and defective inflammation resolution in atherosclerosis. *Nature Reviews Immunology*, **10**(1), 36–46.

Yahagi, Kazuyuki, Kolodgie, Frank D, Otsuka, Fumiyuki, Finn, Aloke V, Davis, Harry R, Joner, Michael, & Virmani, Renu. 2016. Pathophysiology of native coronary, vein graft, and in-stent atherosclerosis. *Nature Reviews Cardiology*, **13**(2), 79–98.